

“Weight Optimization of Active Thermal Management Using a Novel Heat Pump”

Contract number 4507460
Award Number NAG3-2630

Prepared by:

William E. Lear, Principal Investigator
S.A. Sherif, Co-Investigator
University of Florida
Department of Mechanical Engineering
PO Box 116300
Gainesville, FL 32611

Submitted to:

Kenneth D. Mellott
NASA Glenn Research Center
21000 Brookpark Road
Mail Stop 301-2
Cleveland, OH 44135

Introduction

Efficient lightweight power generation and thermal management are two important aspects for space applications. Weight is added to the space platforms due to the inherent weight of the onboard power generation equipment and the additional weight of the required thermal management systems. Thermal management of spacecraft relies on rejection of heat via radiation, a process that can result in large radiator mass, depending upon the heat rejection temperature. For some missions, it is advantageous to incorporate an active thermal management system, allowing the heat rejection temperature to be greater than the load temperature. This allows a reduction of radiator mass at the expense of additional system complexity. A particular type of active thermal management system is based on a thermodynamic cycle, developed by the authors, called the Solar Integrated Thermal Management and Power (SITMAP) cycle. This system has been a focus of the authors' research program in the recent past (see Fig. 1). One implementation of the system requires no moving parts, which decreases the vibration level and enhances reliability. Compression of the refrigerant working fluid is accomplished in this scheme via an ejector.

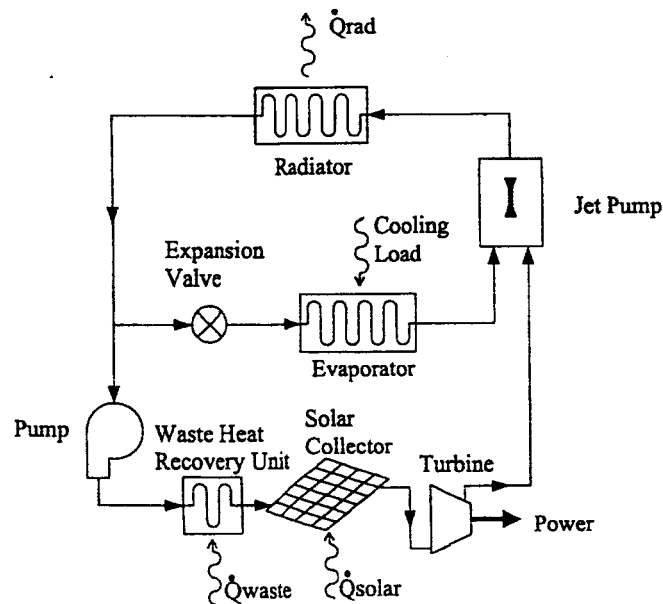


Figure 1. Schematic of the Solar Integrated Thermal Management and Power (SITMAP) cycle

Research work done on the SITMAP cycle is comprised of two parts, an analytical part, and an experimental part. Following are summaries of both parts of the program.

Analytical program

The analytical part went through different stages starting with the development of a computer code (JetSit, which is short for Jet-pump and SITMAP) for the thermodynamic simulation of the cycle. An expression was then needed to measure the mass based performance of the cycle. For that purpose a System Mass Ratio (SMR) expression was derived and incorporated into the simulation code JetSit. Further development of the code involved incorporating thermodynamic properties software to calculate thermodynamic properties instead of the use of a data file. The software used is called REFPROP and was developed by NIST. Recuperation was then included in the SITMAP cycle as an effort to decrease the weight of the system (see Figure 2). Fabri choking is an important phenomenon that might take place in the mixing chamber of the Jet-pump. Fabri choking refers to conditions when the primary flow expands in the mixing chamber constricting the available flow area for the secondary stream, causing it to accelerate. It is possible for the secondary stream to reach sonic velocity, therefore causing the secondary mass flow rate to become independent of downstream conditions. The Fabri choking analysis was included in the JetSit cycle simulation code to make sure that the input entrainment ratios are physically possible.

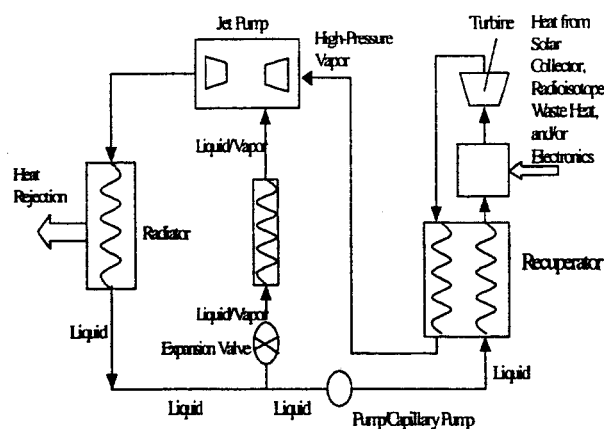


Figure 2. Schematic of the Solar Integrated Thermal Management and Power (SITMAP) cycle with regeneration

The current and most recent stage of the analytical part in the SITMAP program is the optimization of the cycle to minimize the mass for different space missions. To achieve this an optimization program was incorporated in the cycle simulation code. The optimization routine is written by Dr. Leon Lasdon of the University of Texas in Austin and it utilizes a Generalized Reduced Gradient algorithm, and is hence called GRG2.

Results of the analytical part of the program are presented in appendices A and B. Appendix A is the most recently published paper, and appendix B includes the more recent work that has not been published yet, including the Fabri choking and optimization analyses.

Experimental program

The initial consideration in the experimental design process was to conceptually develop the best method of designing an ejector test rig that will be used to study the phenomena of two-phase flow mixing and compression. The primary design criterion established stated that the ejector primary and secondary nozzle inlet states were to be varied over a wide range of pressures, temperatures, and qualities in order to obtain a general database. The wide range of conditions is vital in thoroughly investigating the effects to two-phase flow. A second design requirement dealt with the ability to change the area ratios of the primary and secondary inlet and outlet nozzles. The simulation program JetSit aided in the design of the ejector nozzles.

The first and most important design feature to accommodate was how to vary nozzle inlet states. Conceptually, some kind of loop must be designed to heat and cool the primary and secondary fluid flow. This heating and cooling process would necessarily incorporate the use of one or more heat exchangers. In order to gain control of the pressure, a valve (e.g. adjustable throttling valve) would be needed. The working fluid must also be circulated through the loop; consequently, a pump would be needed. All of the components listed above are basic parts of a system operating on the SITMAP cycle. From this reasoning it was resolved that in order to gain relatively good control of the

experimental apparatus, all components of that system would need to be incorporated. Since it was deemed advantageous to also obtain system-level data for the SITMAP cycle, the choice of ejector rig design was driven towards implementing that cycle directly.

Another important design consideration was the selection of a working fluid for the two-phase flow ejector test rig. The main criterion used in the fluid selection involved the temperature and pressure ranges where the fluid would be in the two-phase region. For safety reasons it was decided that the loop would be operated near ambient temperature and pressure. Information about individual fluids was found by examining their Material Safety Data Sheets (MSDS). Those sheets provide information that cover hazardous ingredients, health effects, handling details, fire and explosion hazard data, first-aid procedures, and critical fluid properties. An important critical fluid property found in the MSDS is the boiling point of a fluid. Since the fluid will be operated in the two-phase region, only fluids with a boiling point temperature slightly above ambient temperature were considered. Based on this information, R-141b was selected. Once the working fluid was selected, the components were sized. Shown below in Figure 3 is a schematic of the final layout of the experimental setup. The most recently published paper on the experimental work is presented in appendix C.

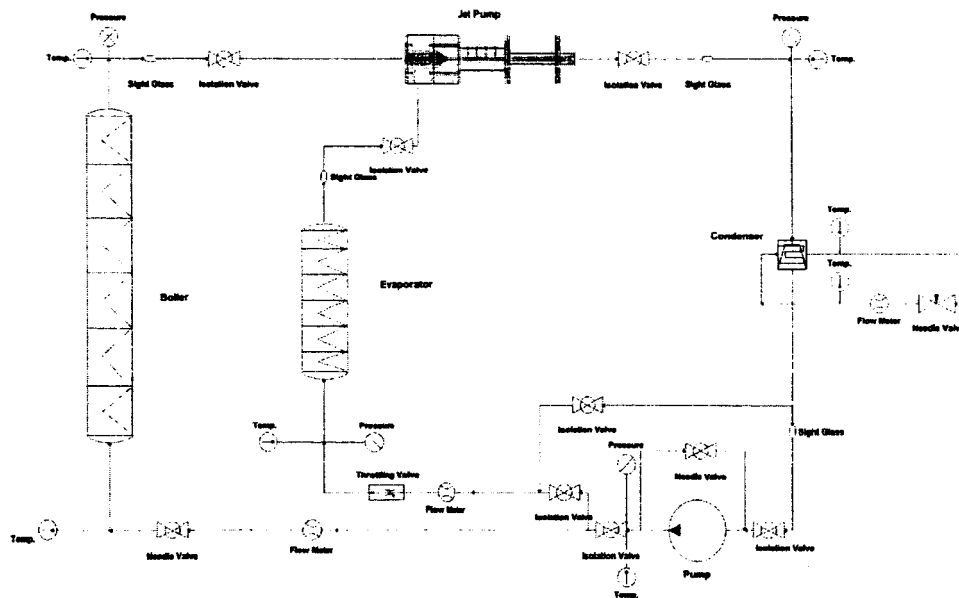


Figure 3. Schematic of the experimental testing apparatus

Appendix A

INTRODUCTION

Efficient lightweight power generation and thermal management are two important aspects for space applications. Weight is added to the space platforms due to the inherent weight of the onboard power generation equipment and the additional weight of the required thermal management systems. In this paper recuperation is included in a novel thermal management and power system as an effort to decrease the weight of the system. The system does not involve any moving parts, which decreases the vibration level and enhances reliability.

The work to be presented in this paper is based on the work done by Nord et al. [1], Freudenberg et al. [2], Kandil et al. [3], and Kandil et al. [4]. Nord et al. [1] developed a combined power and thermal management cycle for onboard spacecraft applications. The cycle is referred to as the Solar Integrated Thermal Management and Power cycle (SITMAP), shown in Figure 1. This cycle is essentially an integrated vapor compression cycle and Rankine cycle with the compression device being a jet pump instead of the regular compressor. The jet pump has several advantages for space applications, as it involves moving parts, which decreases the weight and vibration level while increasing the reliability. The power subsystem is a Rankine cycle, which drives the system. The jet pump acts as the joining device between the thermal and power subsystems, by mixing the high pressure flow from the power subsystem with the low pressure flow from the refrigeration subsystem providing a pressure increase in the refrigeration cycle. Nord et al. [1] used Refrigerant 134-a as the working fluid in their analysis. The mechanical power produced by the turbine can be used to drive the mechanical pump as well as other onboard applications. This allows the SITMAP cycle to be solely driven by solar thermal input.

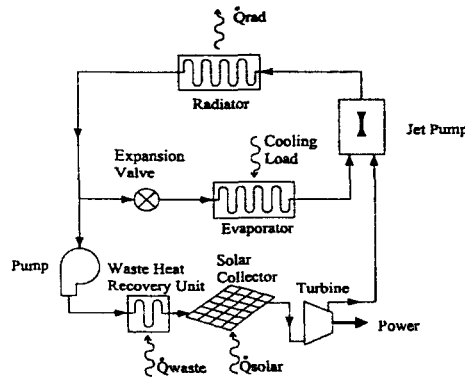


Figure 1. Schematic of the Solar Integrated Thermal Management and Power (SITMAP) cycle

Freudenberg et al. [2], motivated by the novel SITMAP cycle developed by Nord et al. [1], derived an expression for a system mass ratio (SMR) as a mass-based figure of merit for any thermally actuated heat pump with power and thermal management subsystems. SMR is the ratio between the overall system mass to the mass of an ideal passive radiator (where there is no refrigeration subsystem) in which the ideal radiator operates at the same temperature as the cooling load. SMR depends on several dimensionless parameters including three temperature parameters as well as structural and efficiency parameters. Freudenberg et al. [2] estimated the range of each parameter for a typical thermally actuated cooling system operating in space. They

investigated the effect of varying each of the parameters within the estimated range, comparing their analysis to a base model based on the average value of each of the ranges.

Kandil et al. [3] applied the SMR analysis, presented by Freudenberg et al. [2], to the SITMAP cycle developed by Nord et al. [1] to study the effect of different SITMAP input parameters on the overall mass of the system. The inputs to the SITMAP analysis, as presented by Nord et al. [1], are the inlet states for the jet pump and the entrainment ratio, defined as the ratio between the secondary flow (flow rate in the refrigeration loop) to the primary flow (flow rate in the power loop). For this purpose, seven cases were developed for the SITMAP cycle with different values of the five SITMAP parameters. As mentioned earlier, the SMR depends on seven dimensionless parameters. Three of the SMR parameters are dictated by the SITMAP cycle analysis; those parameters are the collector temperature T_{col}^* , radiator temperature T_{rad}^* , and the overall percentage Carnot efficiency ξ_T . The effect of the remaining SMR parameters on the SMR was also investigated. Kandil et al. [3] used liquid nitrogen as the working fluid. One particular advantage for the use of liquid nitrogen is its presence onboard for cooling sensors and imaging systems. Thus, its use as the working fluid will allow for self-cooling as an alternative to conventional cryocoolers, potentially adding a further weight advantage for the SITMAP cycle.

Recent progress has been made by Kandil et al. [4], they incorporated a recuperator within the power subsystem of the SITMAP cycle, shown in Figure 2, allowing the solar collector mass to be significantly reduced. Kandil et al. [4] compared the recuperated cycle to the non-recuperated cycle for the same mission-specific parameters. The mission-specific parameters being the cooling load temperature (the secondary inlet temperature), the technology level (expressed as the ratio of mass per unit area of the heat exchangers), distance from the sun, expressed by the solar constant G_{sun} . The collector temperature (turbine inlet temperature) has also been held constant for comparing the non-recuperated to the recuperated cycle based on the fixed turbine materials limit.

Examples of work relevant to the SITMAP investigation include Bredikhin et al. [8], Cunningham and Dopkin [11], Cunningham [12], Elger et al. [13], Fabri and Paulon [14], Fabri and Siestrunk [15], Fairuzov and Bredikhin [16], Holladay and Hunt [17], Holmes et al. [18], Jiao et al. [19], Lear et al. [22], Marini et al. [23], Neve [24], and Sherif et al. [25]. Literature dealing with thermally actuated cooling systems includes those by Kakabaev and Davletov [20], Chen [10], Lansing and Chai [21], and Chai and Lansing [9]. Many systems dealing with power and thermal management have been proposed for which the System Mass Ratio (SMR) analysis can be used, including absorption cooling systems and solar-powered vapor jet refrigeration systems. Examples of these systems are found in the works of Abrahamsson et al. [5], Alefeld and Radermacher [6], Anderson [7], Chai and Lansing [9], Chen [10], and Lansing and Chai [21].

The purpose of this work is to perform preliminary manual optimization to the recuperated SITMAP cycle to study the effect of different SITMAP input parameters (jet pump primary and secondary inlet states and the entrainment ratio) on the overall mass of the system and see what is the minimum SMR for a specific mission. The optimum recuperated cycle for the given

mission will be compared to a non-recuperated cycle satisfying the same mission requirements pointing out the advantage of recuperation. Liquid nitrogen will be used as the working fluid for the aforementioned advantages.

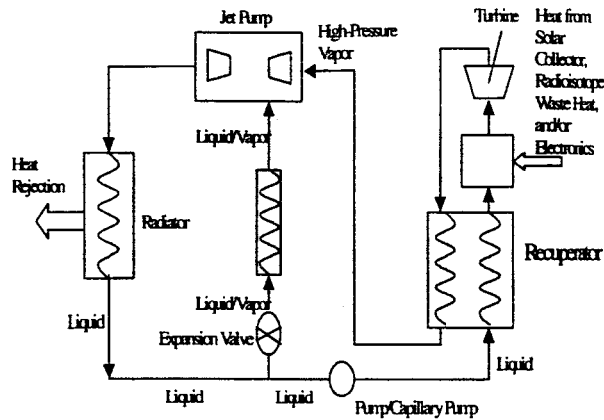


Figure 2. Schematic of the Solar Integrated Thermal Management and Power (SITMAP) cycle with regeneration

ANALYSIS

The analysis used in this work is comprised of the jet pump analysis, the SITMAP cycle analysis, and the system mass ratio analysis. Nord et al. [1] presented a detailed analysis for the jet pump and the SITMAP cycle without recuperation, while Freudenberg et al. [2] discussed the SMR calculation in detail. Nord et al. [1] presented an iterative scheme that solves for the jet pump exit state given the primary and secondary inlet states and the entrainment ratio. They then presented another iterative scheme to solve for all the other states in the SITMAP cycle given the output of the jet pump analysis. The jet pump and the SMR analyses used in this paper are similar to those presented in Nord et al. [1] and Freudenberg et al. [2]. Kandil et al. [4] developed an analysis scheme for the recuperated SITMAP cycle. A brief summary of the SITMAP cycle, and the SMR analyses is included for better understanding of the results presented in this paper. The jet pump analysis is not included and the reader is referred to Nord et al. [1] for a detailed description of that part.

SITMAP Cycle Analysis with Recuperation

Figure 2 shows the modified SITMAP cycle with recuperation. The method used to achieve a converged solution for the SITMAP cycle given the jet pump inlet and exit states and entrainment ratio follows.

Overall analysis.

System convergence requires a double-iterative solution. The first step requires guessing the turbine inlet state (P_{ti} and T_{ti}). Knowing P_{ti} the pump exit pressure P_{pe} can be calculated using the pressure drop ratio across the heat exchangers which is assumed to be $r = 0.97$. The work balance between the turbine and pump can then be used to find the specific enthalpy at the turbine exit, h_{te} , using Equation (1)

$$\dot{W}_p = \dot{W}_T \Rightarrow \frac{\dot{m}_p}{\eta_p \rho_{re}} (P_{pe} - P_{re}) = \dot{m}_p (h_{ti} - h_{te}) \quad (1)$$

The primary inlet pressure P_{pi} can be used with the heat exchangers pressure ratio to get the P_{te} which completely defines the turbine exit state. The definition of the turbine efficiency, Equation (2), is then used to calculate the specific enthalpy of the isentropic turbine exit state, h_{ts}

$$h_{ts} = h_{ti} - \frac{h_{ti} - h_{pi}}{\eta_t} \quad (2)$$

The specific enthalpy from Equation (2) and the fact that $P_{ts} = P_{pi}$ defines the isentropic turbine exit state. Iteration on T_{ti} continues until the entropy corresponding to the current turbine inlet state matches that of the calculated isentropic turbine exit state.

At this point, the correct inlet temperature corresponding to the guessed turbine inlet pressure and the specified turbine efficiency has been obtained. The energy conservation for the Rankine cycle, Equation (3) is then used to solve for the specific enthalpy at the solar collector inlet, h_{sci}

$$h_{ti} - h_{sci} = h_{pi} - h_{re} \quad (3)$$

It should be noted that since there is work balance between the pump and the turbine, the energy balance for the Rankine cycle reduces to Equation (3) which states that the heat input at the solar collector is equal to the difference in enthalpy between the primary inlet and the radiator exit states. The latter is the same as the pump inlet.

The next step is to invoke the overall energy balance, Equation (4), for the whole SITMAP cycle to determine the validity of the guessed turbine inlet pressure.

$$h_{ti} - h_{bi} = (1 + \phi)(h_{jpe} - h_{re}) - \phi(h_{si} - h_{ei}) \quad (4)$$

Iteration on P_{ti} continues (repeat the entire SITMAP analysis) until Equation (4) is satisfied.

A converged solution has now been obtained for the SITMAP cycle. The following equations complete the analysis:

$$h_{pe} = h_{re} + (h_{ti} - h_{pi}) \quad (5)$$

$$h_{ei} = h_{re} \quad (6)$$

$$\dot{Q}_{evap} = \phi \dot{m}_p (h_{si} - h_{ei}) \quad (7)$$

$$\dot{Q}_{rad} = \dot{m}_p (1 + \phi) (h_{de} - h_{re}) \quad (8)$$

$$\dot{Q}_{sc} = \dot{m}_p (h_{ti} - h_{pe}) \quad (9)$$

Note that Equation (9) assumes the worst-case scenario of no waste heat recovery.

The solar collector efficiency was estimated at 80%, and the pump, turbine, and radiator efficiencies were estimated to be 95%. Frictional pressure losses in the system were lumped into an estimated pressure ratio, r , over the various heat exchangers of 0.97.

Solar collector model.

The solar collector was modeled using a solar constant, G_{sun} , of 1353 W/m^2 . Generally, G_{sun} depends on the distance from the sun, which is fixed for a given mission. Equation (10) is used to estimate the area of the solar collector

$$A_{sc} = \frac{\dot{Q}_{sc}}{\eta_{sc} G_{sun}} \quad (10)$$

Radiator model.

Equation (11) represents the energy balance between the fluid and the radiator; the effect of emissivity has been lumped into an overall radiator efficiency, η_{rad} ,

$$dA_{rad} = \frac{-\dot{m}_p}{\eta_{rad} \sigma} T_{rad}^{-4} dh_{rad} \quad (11)$$

If superheat exists at the radiator inlet, Equation (11) must be numerically integrated to account for the decreasing temperature in the superheated region. For saturated flow, Equation (11) can be analytically integrated, using the estimation of constant temperature at an average saturation pressure over the radiator.

To efficiently perform the above calculations and create performance graphs, a program called JetSit was developed by Nord et al.[1]. JetSit's main functions are to calculate the jet pump geometry and diffuser exit state and to use those results to calculate a solution to the SITMAP cycle. It should be noted that JetSit is able to analyze jet pump solutions for all flow regimes, including saturated flow. To perform the analysis in this paper, modifications were made to the JetSit code to be able to change the working fluid to nitrogen, incorporate wider working fluid state regimes, incorporate the SMR analysis, and include recuperation in the power cycle.

System Mass Ratio (SMR) Analysis

Figure 3 shows a schematic for the conceptual thermally actuated heat pump system being considered. The power subsystem accepts heat from a high-temperature source and supplies the power needed by the refrigeration subsystem. Both systems reject heat via a radiator to a common heat sink. The power cycle supplies just enough power internally to maintain and

operate the refrigeration loop. However, in principle, the power cycle could provide power for other onboard systems if needed. Both the power and refrigeration systems are considered generic and can be modeled by any specific type of heat engine such as the Rankine, Sterling, and Brayton cycles for the power subsystem and gas refrigeration or vapor compression cycles for the cooling subsystem.

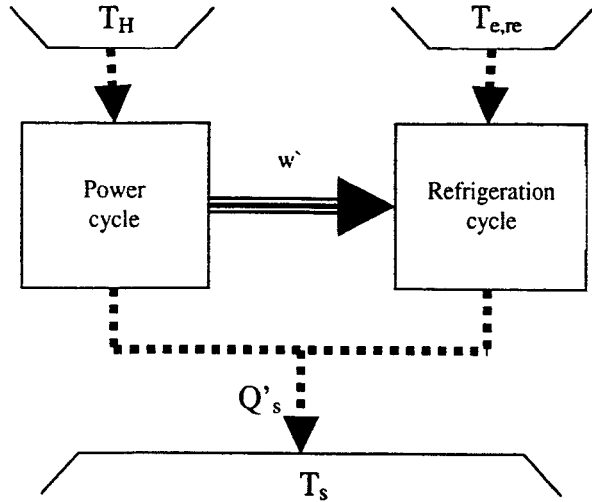


Figure 3. Overall system schematic for SMR analysis

The System Mass Ratio (SMR) is defined as the ratio between the mass of the overall system and that of an idealized passive system. The overall system mass is divided into three terms; radiator, collector, and a general system mass comprising the turbomachinery and piping present in an active system. This is shown mathematically by

$$\tilde{m} = \frac{m_{col} + m_{rad} + m_{sys}}{m_{rad,o}} \quad (12)$$

Freudenberg et al. [2] showed that the above equation can be expressed as follows:

$$\tilde{m} = \frac{1}{\epsilon(1-\mu)} \left\{ \frac{T_{col}^4(T_{rad}^4 - 1)(1 - T_s^4)}{\xi(T_{col}^4 - T_{rad}^4)} \left[\zeta + \left(\frac{1}{T_{rad}^4 - T_s^4} \right) \right] + \left(\frac{1 - T_s^4}{T_{rad}^4 - T_s^4} \right) \right\} \quad (13)$$

where

$$\eta = \frac{w'}{Q_H} ; COP = \frac{Q_c}{w'} ; \eta COP = \frac{Q_c}{Q_H} \quad (14)$$

$$\xi_p = \frac{\eta}{\eta_c} ; \xi_R = \frac{COP}{COP_c} ; \xi_T = \xi_p \xi_R \quad (15)$$

$$\eta_c = 1 - \frac{T_{rad}}{T_{col}} ; COP_c = \frac{T_c}{T_{rad} - T_c} \quad (16)$$

$$\mu = \frac{m_{sys}}{m_{t,act}}; \alpha = \frac{\lambda_{col}}{\lambda_{rad}}; \zeta = \frac{\alpha \epsilon \sigma T_c^4}{\eta_{col} G_{sun}} \quad (17)$$

$$T_{col}^* = \frac{T_{col}}{T_c}; T_{rad}^* = \frac{T_{rad}}{T_c}; T_s^* = \frac{T_s}{T_c} \quad (18)$$

Equation (13) represents the SMR in terms of seven system parameters. Three of these parameters are based on temperature ratios and the remaining four are based on system properties. All of the parameters are quantities that can be computed for a given application. It should be noted that for a specific mission the value of T_c (cooling load temperature) is fixed.

In the analysis involved in this paper the emissivity, ϵ was held constant at 0.865, the mass ratio, μ at 0.5, the ratio of mass per unit area α at 0.18, the collector efficiency η_{col} at 0.8, and the sun constant G_{sun} at 1383 W/m^2 .

RESULTS AND DISCUSSION

Kandil et al. [3] studied the effect of each of the five input parameters to the SITMAP cycle analysis as implemented in the JetSit code, namely the primary jet pump inlet temperature and pressure, the secondary jet pump inlet temperature and pressure, and the entrainment ratio. They performed the SMR analysis on eight cases, where Case 1 was the base case for comparison and each of the other seven cases demonstrated the effect of each of the five parameters by changing its value while maintaining all other parameters at their base values.

Kandil et al. [4] studied the effect of recuperation on the overall SMR. For this purpose only two cases are studied. Case 1 is the standard SITMAP cycle studied by Nord et al.[1] and Kandil et al.[3] (Figure 1), and Case 2 is the modified SITMAP cycle with recuperation (Figure 2). The challenge in comparing the two cycles lies in determining the basis of comparison because the cycles are thermodynamically different. The first comparison is made fixing the primary and secondary jet pump inlet states, and the entrainment ratio, for both cycles. They showed that, for the same jet pump inlet conditions and entrainment ratio, the SMR for both cycles is almost identical. This result is not what would normally be expected, because the recuperation is supposed to lower the system mass ratio. This is due to the fact that fixing the jet pump inlet conditions for both cycles overly constrains the analysis because it fixes all the states in the refrigeration part of both cycles. This leaves only two terms in the SMR expression to vary between the two cycles, namely the normalized collector temperature, T_{col}^* , and the percentage Carnot efficiency, ξ_T . However, the change in the value of those two parameters was not enough to cause a significant change in the SMR values between Cases 1 and 2 to show the effect of recuperation on the cycle performance.

The second comparison made between the two cycles, fixing the evaporator exit temperature (secondary inlet temperature), and the turbine inlet temperature for both cycles and allowing the other jet pump inlet states to vary. This is a more realistic constraint for most applications, since materials limit the turbine inlet temperature for many cycles and the secondary inlet temperature

is a mission-specific parameter that should be held fixed for fair comparison of both cycles. Results of this comparison showed the advantage of recuperation.

However, the interest in this paper is to perform preliminary optimization of the recuperated cycle for a given mission by varying the input parameters to yield a minimum SMR for that mission. However, it should be noted that one of the five input parameters, namely, the secondary inlet temperature, is fixed because it is one of the mission specific parameters. Table 1 shows the optimization results for the recuperated cycle. The mission cooling load temperature, T_{si} was fixed at $-175\text{ }^{\circ}\text{C}$, while the normalized turbine inlet temperature (normalized collector temperature), T_{col}^* at around 3.2. The optimization was carried out by varying each of the four input parameters, namely, the primary inlet temperature and pressure, the secondary inlet pressure, and the entrainment ratio. Each of the parameters was varied independently in the direction of decreasing system mass ratio from its value at case 1 which is the base case. Cases 1 through 5 show that increasing the primary and secondary inlets pressures decreases the SMR. Case 6 is a new base case that combines the optimum values for the parameters that has been varied in cases 1 through 5, thus it shows a lower SMR than the first five cases. Cases 6 through 9 show that lowering the primary inlet temperature, T_{si} and increasing the entrainment ratio, ϕ helped reduce the SMR significantly. Case 9 can be considered the optimum for the given mission, because non of the variables could be changed any further to yield lower values of the SMR. Any further increase in ϕ or decrease in T_{pi} yielded a radiator exit temperature that was lower than the mission-specified T_{si} , which of course cannot be the case, because then there would be no need for the refrigeration cycle. The value of P_{si} is limited by P_{sat} (at $T_{si} = -175\text{ }^{\circ}\text{C}$) = 0.66 MPa, because if P_{si} was less than P_{sat} , then the secondary inlet state would be subcooled which is not possible.

To show the effect of recuperation, a set of cases were calculated for the non-recuperated SITMAP cycle, shown in Table 2, for the sake of comparison. Cases 1 through 9 have exactly the same input parameters as cases 1 through 9 in table 1, for the recuperated cycle. As mentioned earlier, constraining the comparison for the same input parameters yielded identical SMR values for both the recuperated and the non-recuperated cycles, as was concluded by Kandil et al. [3]. Case 10 shows the more physical comparison to Case 9 in Table 1, with fixed T_{si} , and T_{col}^* . Comparing these two cases shows a significant advantage for the recuperated cycle over the non-recuperated one for a specific mission.

CONCLUSIONS

This paper examined the effect of recuperation on the mass-based parameter, SMR to determine an optimum recuperated cycle, and the advantage of recuperated systems, based on weight and economic savings. With the use of this mass parameter, an preliminary optimization was performed for a recuperated SITMAP cycle, and a comparison between recuperated and non-recuperated SITMAP cycles was made to determine conditions under which recuperated cycles possess an advantage based on mass savings over their non-recuperated counterparts. The comparison was made based on specified secondary jet pump inlet temperature as well as a specified turbine inlet temperature. The following conclusions can be drawn regarding these comparisons:

- The overall mass advantage for recuperated systems increases with increasing values of the primary and secondary inlet pressures, and the entrainment ratio.
- The overall mass advantage for recuperated systems increases with decreasing values of the primary inlet temperature.
- the recuperated cycle has a significant advantage over the non-recuperated one for a specific mission, and a specific turbine inlet temperature.

It follows from the above conclusions that, for the configuration and ranges studied, particular recuperated systems can in fact have a significant reduction of mass over non-recuperated systems. Estimation of the values of the different parameters may be made during the preliminary design phase of a space mission, allowing an early choice to be made between recuperated and non-recuperated thermal management systems. This should simplify and streamline the design process.

ACKNOWLEDGMENTS

This work was partially supported by NASA Glenn Research Center under grant number NRA-01-GRC-1 in the area of space power technology. Support from the Department of Mechanical Engineering at the University of Florida is also gratefully acknowledged.

REFERENCES

- [1] Nord, J.W., Lear, W.E., and Sherif, S.A., "Design Analysis of a Heat-Driven Jet Pumped Cooling System for Space Thermal Management Applications," *AIAA Journal of Propulsion and Power*, Vol. 17, No. 3, pp. 566-570.
- [2] Freudenberg, K., Lear, W. E., and Sherif, S. A., "Parametric Analysis of a Thermally Actuated Cooling System for Space Applications," *Proceedings of the ASME Advanced Energy Systems Division*, AES-Vol. 40, November 2000, pp. 499-510.
- [3] Kandil, S., Lear, W.E., and Sherif, S.A., "Performance of Jet-Pumped Cryogenic Refrigeration System." *40th AIAA Aerospace Sciences Meeting and Exhibit*, Reno, Nevada, January 14-17, 2002, AIAA Paper 2002-1031.
- [4] Kandil, S., Lear, W. E., and Sherif, S. A., "Mass Advantages in a Jet-Pumped Active Thermal Management System." *SAE Power Systems Conference*, Coral Springs, Florida,
- [5] Abrahamsson, K., Jernqvist, A., and Ally, G., "Thermodynamic Analysis of Absorption Heat Cycles," *Proc. of the International Absorption Heat Pump Conference*, New Orleans, Louisiana, AES-Vol. 31, ASME, 1994, pp. 375-383.
- [6] Alefeld, G. and Radermacher, R., *Heat Conversion Systems*, CRC Press, Boca Raton, Florida, 1994.

- [7] Anderson, H., "Assessment of Solar Powered Vapor Jet Air-conditioning System," *International Solar Energy Congress and Exposition (ISES)*, Los Angeles, California, pp. 408, 1975.
- [8] Bredikhin, V.V., Gorbenko, G.A., Nikonov, A.A., and Fairuzov, Y.V., "Mathematical Modeling of Thermo-Circulating Loops with Jet Pumps," *Hydrodynamic Processes in Multi-Phase Working Fluid Energy Plants*, Kharkov Aviation Institute, Kharkov, Ukraine, pp. 3-10 (in Russian), 1990.
- [9] Chai, V.W. and Lansing, F.L., "A Thermodynamic Analysis of a Solar-powered Jet Refrigeration System," DSN Progress Report 41-42, Jet Propulsion Laboratory, 1977, pp. 209-217.
- [10] Chen, L.T., "Solar Powered Vapor-Compressive Refrigeration System Using Ejector as the Thermal Compressors," *Proceedings of the National Science Council*, No. 10, Part 3, pp. 115-132, 1977.
- [11] Cunningham, R.G. and Dopkin, R.J., "Jet Breakup and the Mixing Throat Lengths for the Liquid Jet Pump," *ASME Journal of Fluids Engineering*, Vol. 96, No. 3, pp. 216-226, 1974.
- [12] Cunningham, R.G., "Liquid Jet Pumps for Two-Phase Flows," *ASME Journal of Fluids Engineering*, Vol. 117, No. 2, pp. 309-316, 1995.
- [13] Elger, D.F., McLam, E.T., and Taylor, S.J., "A New Way to Represent Jet Pump Performance," *ASME Journal of Fluids Engineering*, Vol. 113, No. 3, pp. 439-444, 1991.
- [14] Fabri, J. and Paulon, J., "Theory and Experiments on Air-to-Air Supersonic Ejectors," NACA-TM-1410, September 1958.
- [15] Fabri, J. and Siestrunk, R., "Supersonic Air Ejectors," *Advances in Applied Mechanics*, Vol. V, H.L. Dryden and Th. von Karman (editors), Academic Press, New York, 1958, pp. 1-33.
- [16] Fairuzov, Y.V. and Bredikhin, V.V., "Two Phase Cooling System with a Jet Pump for Spacecraft," *AIAA Journal of Thermophysics and Heat Transfer*, Vol. 9, No. 2, April-June 1995, pp. 285-291.
- [17] Holladay, J.B. and Hunt, P.L., "Fabrication, Testing, and Analysis of a Flow Boiling Test Facility with Jet Pump and Enhanced Surface Capability," Research Proposal, NASA Marshall Space Flight Center, Thermal and Life Support Division, Huntsville, Alabama, 1996.
- [18] Holmes, H.R., Geopp, J., and Hewitt, H.W., "Development of the Lockheed Pumped Two Phase Thermal Bus," AIAA Paper 87-1626, June 1987.

- [19] Jiao, B., Blais, R.N., and Schmidt, Z., "Efficiency and Pressure Recovery in Hydraulic Jet Pumping of Two-Phase Gas/Liquid Mixtures," *SPE Production Engineering*, Vol. 5, No.4, 1990, pp. 361-364.
- [20] Kakabaev, A. and Davletov, A., "A Freon Ejector Solar Cooler," *Geliotekhnika*, Vol. 2, No. 5, September 1966, pp. 42-48.
- [21] Lansing, F.L. and Chai, V.W., "Performance of Solar-Powered Vapor-Jet Refrigeration Systems with Selected Working Fluids," DSN Progress Report 42-44, Jet Propulsion Laboratory, 1978, pp. 245-248.
- [22] Lear, W.E., Sherif, S.A., Steadham, J.M., Hunt, P.L., and Holladay, J.B., "Design Considerations of Jet Pumps with Supersonic Two-Phase Flow and Shocks," *AIAA 37th Aerospace Sciences Meeting*, Reno, Nevada, January 11-14, AIAA Paper 99-0461, 1999.
- [23] Marini, M., Massardo, A., Satta, A., and Geraci, M., "Low Area Ratio Aircraft Fuel Jet-Pump Performance with and without Cavitation," *ASME Journal of Fluids Engineering*, Vol. 114, No. 4, 1992, pp. 626-631.
- [24] Neve, R.S., "Diffuser Performance in Two-Phase Jet Pump," *International Journal of Multiphase Flow*, Vol. 17, No. 2, pp. 267-272, 1991.
- [25] Sherif, S.A., Lear, W.E., Steadham, J.M., Hunt, P.L., and Holladay, J.B., "Analysis and Modeling of a Two-Phase Jet Pump of a Thermal Management System for Aerospace Applications," *International Journal of Mechanical Sciences*, Vol. 42, No. 2, February 2000, pp. 185-198.

Table 1: Recuperated cycle cases

| Case | T_{pi} | P_{pi} | T_{si} | P_{si} | ϕ | ηCOP | Q_{eavp} | Q_{rad} | Q_{recup} | Q_{waste} | T^*_{col} | T^*_{rad} | ξ_T | SMR | P_r |
|------|----------|----------|----------|----------|--------|------------|------------|-----------|-------------|-------------|-------------|-------------|---------|------|-------|
| 1 | -80 | 4 | -175 | 0.4 | 2 | 1.33 | 341.2 | 596.5 | 136.6 | 255.3 | 3.24 | 1.00 | 0.007 | 5.29 | 1.8 |
| 2 | -80 | 8 | -175 | 0.4 | 2 | 1.46 | 339.8 | 572.3 | 145.5 | 232.6 | 3.27 | 1.01 | 0.014 | 4.99 | 1.9 |
| 3 | -80 | 10 | -175 | 0.4 | 2 | 1.52 | 336.3 | 557.1 | 153.3 | 220.8 | 3.31 | 1.01 | 0.032 | 4.77 | 2 |
| 4 | -80 | 4 | -175 | 0.5 | 2 | 1.32 | 336.8 | 592.2 | 136.7 | 255.4 | 3.24 | 1.00 | 0.006 | 5.34 | 1.5 |
| 5 | -80 | 4 | -175 | 0.6 | 2 | 1.29 | 323.8 | 575 | 135.5 | 251.2 | 3.23 | 1.02 | 0.041 | 5.13 | 1.4 |
| 6 | -80 | 10 | -175 | 0.6 | 2 | 1.47 | 317.8 | 534 | 147.1 | 216.2 | 3.26 | 1.03 | 0.074 | 4.58 | 1.5 |
| 7 | -80 | 10 | -175 | 0.6 | 4 | 2.97 | 665 | 888.5 | 151 | 223.5 | 3.29 | 1.00 | 0.01 | 3.65 | 1.2 |
| 8 | -90 | 10 | -175 | 0.6 | 4 | 3.24 | 665.6 | 871 | 169.2 | 205.4 | 3.29 | 1.00 | 0.008 | 3.55 | 1.2 |
| 9 | -100 | 10 | -175 | 0.6 | 4 | 3.6 | 666.2 | 851.2 | 189.7 | 185 | 3.29 | 1.00 | 0.005 | 3.43 | 1.2 |

Table 2: Non-recuperated cycle cases

| Case | T_{pi} | P_{pi} | T_{si} | P_{si} | ϕ | ηCOP | Q_{eavp} | Q_{rad} | Q_{waste} | T^*_{col} | T^*_{rad} | ξ_T | SMR | P_r |
|------|----------|----------|----------|----------|--------|------------|------------|-----------|-------------|-------------|-------------|---------|------|-------|
| 1 | -80 | 4 | -175 | 0.4 | 2 | 1.33 | 341.2 | 596.5 | 255.3 | 2.04 | 1.00 | 0.009 | 5.29 | 1.8 |
| 2 | -80 | 8 | -175 | 0.4 | 2 | 1.46 | 339.8 | 572.3 | 232.6 | 2.17 | 1.01 | 0.018 | 4.99 | 1.9 |
| 3 | -80 | 10 | -175 | 0.4 | 2 | 1.52 | 336.3 | 557.1 | 220.8 | 2.25 | 1.01 | 0.04 | 4.77 | 2 |
| 4 | -80 | 4 | -175 | 0.5 | 2 | 1.32 | 336.8 | 592.2 | 255.4 | 2.04 | 1.00 | 0.008 | 5.34 | 1.5 |
| 5 | -80 | 4 | -175 | 0.6 | 2 | 1.29 | 323.8 | 575 | 251.2 | 2.04 | 1.02 | 0.056 | 5.13 | 1.4 |
| 6 | -80 | 10 | -175 | 0.6 | 2 | 1.47 | 317.8 | 534 | 216.2 | 2.26 | 1.03 | 0.093 | 4.58 | 1.5 |
| 7 | -80 | 10 | -175 | 0.6 | 4 | 2.97 | 665 | 888.5 | 223.5 | 2.25 | 1.00 | 0.013 | 3.65 | 1.2 |
| 8 | -90 | 10 | -175 | 0.6 | 4 | 3.24 | 665.6 | 871 | 205.4 | 2.18 | 1.00 | 0.01 | 3.55 | 1.2 |
| 9 | -100 | 10 | -175 | 0.6 | 4 | 3.6 | 666.2 | 851.2 | 185 | 2.12 | 1.00 | 0.007 | 3.43 | 1.2 |
| 10 | 0 | 14 | -175 | 0.6 | 0.5 | 0.2 | 54 | 324.1 | 270.1 | 3.22 | 1.22 | 0.07 | 15.1 | 4.2 |

Appendix B

Fabri choking analysis

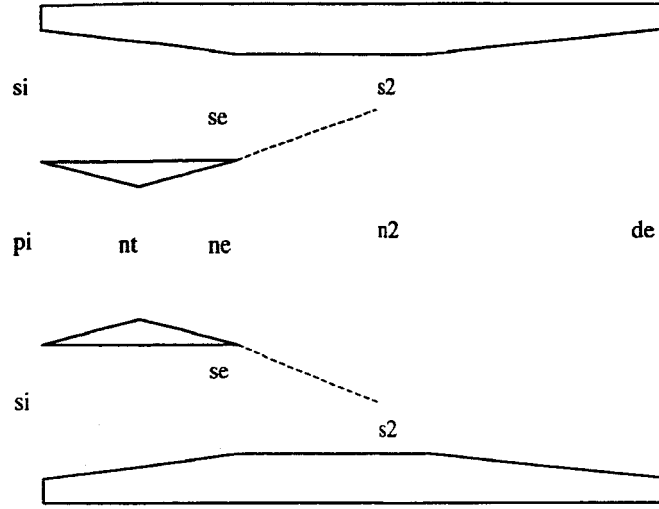


Figure 1. Schematic for the Jet-pump with constant area mixing, showing the Fabri choked state s2.

The momentum equation for the control volume over the mixing chamber can be written as

$$P_{se}A_{se} + P_{ne}A_{ne} - P_{s2}A_{s2} - P_{n2}A_{n2} = \dot{m}_p V_{n2} + \dot{m}_s V_{s2} - \dot{m}_p V_{ne} - \dot{m}_s V_{se} \quad (1a)$$

dividing by \dot{m}_p yields

$$\frac{1}{\dot{m}_p} (P_{se}A_{se} + P_{ne}A_{ne} - P_{s2}A_{s2} - P_{n2}A_{n2}) = (V_{n2} - V_{ne}) + \phi_{Fabri} (V_{s2} - V_{se}) \quad (1b)$$

$$\therefore \phi_{Fabri} = \frac{(P_{se}A_{se} + P_{ne}A_{ne} - P_{s2}A_{s2} - P_{n2}A_{n2})}{\dot{m}_p (V_{s2} - V_{se})} - \frac{(V_{n2} - V_{ne})}{(V_{s2} - V_{se})} \quad (1c)$$

$$\therefore \phi_{Fabri} = \frac{\left(P_{se} + P_{ne} \frac{A_{ne}}{A_{se}} - P_{s2} \frac{A_{s2}}{A_{se}} - P_{n2} \frac{A_{n2}}{A_{se}} \right)}{\rho_{ne} V_{ne} \frac{A_{ne}}{A_{se}} (V_{s2} - V_{se})} - \frac{(V_{n2} - V_{ne})}{(V_{s2} - V_{se})} \quad (1d)$$

The iteration scheme starts by guessing a value for P_{se} , knowing that $s_{se} = s_{si}$, that defines the state (se). From the energy equation

$$V_{se} = [2(h_{si} - h_{se})]^{1/2} \quad (2)$$

then ϕ_{Fabri} can be calculated as

$$\phi_{Fabri} = \frac{\rho_{se} V_{se} A_{se}}{\rho_{ne} V_{ne} A_{ne}} \quad (3)$$

It should be noted that the area ratio A_{ne}/A_{se} is an input to the SITMAP code.

Then a guess is made for P_{s2} , and $s_{s2} = s_{se}$, that defines the state (s2). The velocity V_{s2} can be obtained from the energy equation between se and s2

$$V_{s2} = \left[2 \left(h_{se} - h_{s2} + \frac{V_{se}^2}{2} \right) \right]^{1/2} \quad (4)$$

calculate $M_{s2} = \frac{V_{s2}}{a_{s2}}$, and check if it is equal to 1. If not another value for P_{s2} is guessed

till $M_{s2} = 1$.

The area ratio A_{s2}/A_{se} can be calculated from the continuity equation between se and s2,

$$\frac{A_{s2}}{A_{se}} = \frac{\rho_{se} V_{se}}{\rho_{s2} V_{s2}} \quad (5)$$

knowing that for constant-area mixing $A_{ne} + A_{se} = A_{s2} + A_{n2}$, then

$$\frac{A_{n2}}{A_{ne}} = 1 + \frac{A_{se}}{A_{ne}} - \left(\frac{A_{s2}}{A_{se}} \frac{A_{se}}{A_{ne}} \right) \quad (6)$$

From equation 1d another value for ϕ_{Fabri} can be obtained. Iterate on P_{se} till the values for ϕ_{Fabri} from equations (1d) and (3) match.

ϕ_{Fabri} is the maximum possible entrainment ratio for a given geometry and inlet states.

Therefore the simulation code JetSit sets $\phi = \phi_{Fabri}$, if the input value is greater than

ϕ_{Fabri} .

Optimization analysis

As mentioned before the optimization analysis is performed by incorporating a Generalized Reduced Gradient algorithm into the simulation code. The optimization algorithm is written by Dr, Leon Lasdon of the University of Texas in Austin, and is called GRG2.

All the input variables to the simulation program JetSit are the variables in the optimization process. A list of these variables is

- Jet-pump primary inlet pressure
- Jet-pump primary inlet secondary property (entropy, enthalpy, or density)
- Jet-pump secondary inlet pressure
- Jet-pump secondary inlet secondary property (entropy, enthalpy, or density)
- Jet-pump entrainment ratio, ϕ
- Area ratio A_{nt}/A_{ne} in the jet-pump primary nozzle
- Area ratio A_{ne}/A_{se} in the jet-pump
- Turbine inlet pressure

The constraints on the optimization process are

- $P_{ti} - P_{te} > 0$
- $P_{pe} - P_{re} > 0$
- $P_{pi} - P_{si} > 0$
- $P_{jpe} - P_{se} > 0$
- $Q_{evap} > 0$
- $Q_{boiler} > 0$
- $Q_{cond} > 0$
- $SMR > 0$ (objective function, to be minimized)

The objective function is the SMR, which is to be minimized for space applications. All the optimization variables are changed within a specified range to obtain the minimum value for the objective function, SMR, provided all the aforementioned constraints are satisfied.

Appendix C

FEDSM2003-45703

EXPERIMENTAL STUDY OF A CONSTANT-AREA EJECTOR WITH TWO-PHASE FLUIDS

J. A. Bray, W. E. Lear, and S. A. Sherif

Department of Mechanical and Aerospace Engineering

University of Florida

237 MAEB Bldg., P.O. Box 116300

Gainesville, Florida 32611-6300

Tel (352) 392-7821

Fax (352) 392-1071

E-mail: sasherif@ufl.edu

ABSTRACT

The authors are presently involved in developing a design code to optimize an active space thermal management system that includes as a key component an ejector, which operates with fluids in the two-phase regime. In order to validate this code, and for other applications of two-phase ejectors, a comprehensive experimental data set is needed for this device. This paper deals with the conceptual design and implementation of a constant-area ejector experimental rig intended to provide the required data set. The system has been designed to implement the same thermodynamic cycle as the proposed thermal management system, allowing a preliminary performance database to be developed upon testing, in addition to the ejector data. The ejector itself will be an interchangeable part in this system, allowing geometrical variables to be manipulated.

INTRODUCTION

Thermal management of spacecraft relies on rejection of heat via radiation, a process that can result in large radiator mass, depending upon the heat rejection temperature. For some missions, it is advantageous to incorporate an active thermal management system, allowing the heat rejection temperature to be greater than the load temperature. This allows a reduction of radiator mass at the expense of additional system complexity. A particular type of active thermal management system is based on a thermodynamic cycle, developed by the authors, called the Solar Integrated Thermal Management and Power (SITMAP) cycle. This system has been a focus of the authors' research program in the recent past (see Fig. 1). The system requires no moving parts, which decreases the vibration level and enhances reliability. Compression of the refrigerant working fluid is

accomplished in this scheme via an ejector. However, a key uncertainty, addressed in the current paper, is the design of the ejector to accommodate the two-phase flow, which occurs in many operating regimes of interest within the device.

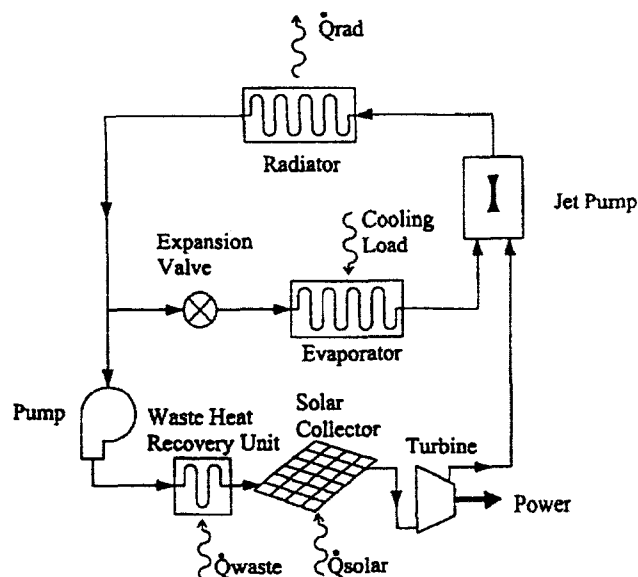


Figure 1. Schematic of the Solar Integrated Thermal Management and Power (SITMAP) cycle

Ejectors have been used in a wide variety of applications for over a century. Examples of applications for ejectors include vacuum pumps in the food industry, power stations, and in the chemical industry; ejector systems used in the aircraft industry for thrust augmentation; and steam-jet ejectors used in refrigeration. The ejector, shown schematically in Fig. 2, has

the advantages of simplicity, no moving parts, low cost, and reliability. Other advantages of the ejector are decreases in both vibration and weight.

Literature dealing with ejectors is abundant, especially when dealing with single-phase flow. Single-phase ejectors exhibit a wide range of fluid phenomena and have historically incorporated the use of empirical methods in their design. However, for the case of two-phase flow in ejectors, there is little information readily available. More information about two-phase ejectors can be found in the works of Sherif et al. [1]. More research is needed in this area to be able to understand and design the ejector component, which would enable the potential mass savings of the SITMAP system.

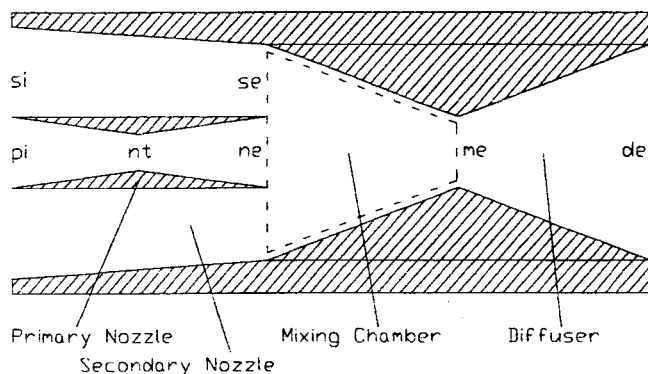


Figure 2. Schematic of ejector (non-constant area mixing)

The work to be presented in this paper is based on research conducted by Nord et al. [2], Freudenberg et al. [3], and Kandil et al. [4]. Nord et al. [2] developed the combined power and thermal management cycle for onboard spacecraft applications referred to above (i.e. SITMAP cycle). This is essentially an integrated vapor compression cycle and a Rankine cycle with the compression device being an ejector instead of the regular compressor. The power subsystem is a Rankine cycle, which drives the system. The ejector acts as the joining device between the thermal and power subsystems, by mixing the high-pressure flow from the power subsystem with the low-pressure flow from the refrigeration subsystem providing a pressure increase in the latter. Nord et al. [2] used Refrigerant 134-a as the working fluid in their analysis. The mechanical power produced by the turbine can be used to drive the mechanical pump as well as other onboard applications. This allows a system operating on the SITMAP cycle to be solely driven by solar thermal input.

Examples of work relevant to the SITMAP investigation include Bredikhin et al. [5], Cunningham and Dopkin [6], Cunningham [7], Elger et al. [8], Fabri and Paulon [9], Fabri and Siestrunk [10], Fairuzov and Bredikhin [11], Holladay and Hunt [12], Holmes et al. [13], Jiao et al. [14], Lear et al. [15], Marini et al. [16], Neve [17] and Sherif et al. [1]. Literature dealing with thermally actuated cooling systems includes those by Kakabaev and Davletov [18], Chen [19], Lansing and Chai [20], and Chai and Lansing [21]. Many systems dealing with power and thermal management have been proposed for which the System Mass Ratio (SMR) analysis developed by Freudenberg et al [3] can be used, including absorption cooling

systems and solar-powered vapor jet refrigeration systems. Examples of those systems are found in the works of Abrahamsson et al. [22], Alefeld and Radermacher [23], Anderson [24], Chai and Lansing [21], Chen [19], and Lansing and Chai [20].

This paper deals with an experimental investigation of a novel active thermal management system that we have proposed for use in space due to its potential for low weight and high reliability. Accordingly, this paper will present the design of an experimental facility for measuring the performance of constant-area ejectors with two-phase flow. Significant modeling has been performed in order to design this device, and the modeling approach will be described, along with the design choices in the construction of the facility. The purpose of the experimental investigation is two fold: to develop an experimental data set for two-phase ejectors (the key uncertainty in designing the proposed thermal management system) and to develop a proof-of-concept experiment for the thermal management system itself. The experimental results will be used to both calibrate the aforementioned model and also provide a high-quality design database of the global performance parameters of two-phase ejectors.

NOMENCLATURE

Latin Symbols

| | |
|-----------|--------------------------------------|
| A | cross-sectional area, m ² |
| D | diameter |
| h | specific enthalpy, kJ/kg |
| m | mass, kg |
| \dot{m} | mass flow rate, kg/s |
| P | pressure, MPa |
| P_r | compression ratio |
| T | temperature, °C |
| V | velocity, m/s |

Greek Symbols

| | |
|--------|--|
| ϕ | entrainment ratio, \dot{m}_s / \dot{m}_p |
|--------|--|

Subscripts

| | |
|----|-----------------------|
| de | diffuser exit |
| me | mixing chamber exit |
| ne | primary nozzle exit |
| nt | primary nozzle throat |
| p | primary flow |
| pi | primary nozzle inlet |
| s | secondary flow |
| se | secondary flow exit |
| si | secondary flow inlet |

EXPERIMENTAL DESIGN

The initial consideration in the experimental design process was to conceptually develop the best method of designing an ejector test rig that will be used to study the phenomena of two-phase flow mixing and compression. The primary design criterion established stated that the ejector

primary and secondary nozzle inlet states were to be varied over a wide range of pressures, temperatures, and qualities in order to obtain a general database. The wide range of conditions is vital in thoroughly investigating the effects to two-phase flow. A second design requirement dealt with the ability to change the area ratios of the primary and secondary inlet and outlet nozzles. The computer program JetSit, written by Nord et al. [2], aided in the design of the ejector nozzles. JetSit, described below, is a computer program designed to model the SITMAP cycle and calculate the key ejector geometry parameters.

The first and most important design feature to accommodate was how to vary nozzle inlet states. Conceptually, some kind of loop must be designed to heat and cool the primary and secondary fluid flow. This heating and cooling process would necessarily incorporate the use of one or more heat exchangers. In order to gain control of the pressure, a valve (e.g. adjustable throttling valve) would be needed. The working fluid must also be circulated through the loop; consequently, a pump would be needed. All of the components listed above are basic parts of a system operating on the SITMAP cycle. From this reasoning it was resolved that in order to gain relatively good control of the experimental apparatus, all components of that system would need to be incorporated. Since it was deemed advantageous to also obtain system-level data for the SITMAP cycle, the choice of ejector rig design was driven towards implementing that cycle directly.

Another important design consideration was the selection of a working fluid for the two-phase flow ejector test rig. The main criterion used in the fluid selection involved the temperature and pressure ranges where the fluid would be in the two-phase region. For safety reasons it was decided that the loop would be operated near ambient temperature and pressure. Information about individual fluids was found by examining their Material Safety Data Sheets (MSDS). Those sheets

provide information that cover hazardous ingredients, health effects, handling details, fire and explosion hazard data, first-aid procedures, and critical fluid properties. An important critical fluid property found in the MSDS is the boiling point of a fluid. Since the fluid will be operated in the two-phase region, only fluids with a boiling point temperature slightly above ambient temperature were considered. Based on this information, R-141b was selected.

Experimental Setup

Once the working fluid was selected, the components were sized. Shown below in Fig. 3 is a schematic of the final layout of the experimental setup. It should be noted that both the boiler and evaporator have a controlled, measurable, and variable heat input. The heat input to the boiler can be varied from 0 to 5 kW, while that to the evaporator can be varied from 0 to 3.3 kW. This allows the ejector's primary and secondary inlets to be varied over a wide range of temperatures and/or qualities. It should also be noted that the pump design incorporates a bypass loop. This loop allows the pump to be operated at different speeds without changing the total mass flow rate through the rest of the piping system. Varying the pump speed allows the primary nozzle inlet pressure (P_{pi}) to be varied directly. The addition of the bypass loop also gives us the capability to vary the secondary nozzle inlet pressure (P_{si}) over a larger range. With this configuration, P_{pi} can be varied over a range of 0.5 MPa to 0.83 MPa, while P_{si} can be varied over the range of 0.15 MPa to 0.5 MPa. The condenser shown in Fig. 3 is a water-cooled condenser. The use of a condenser assures that the refrigerant at the pump inlet is always liquid. The charge or amount of refrigerant in the system is also adjustable. Different charge levels produce different mass flow rates and the pressures at all state points except during the phase change processes.

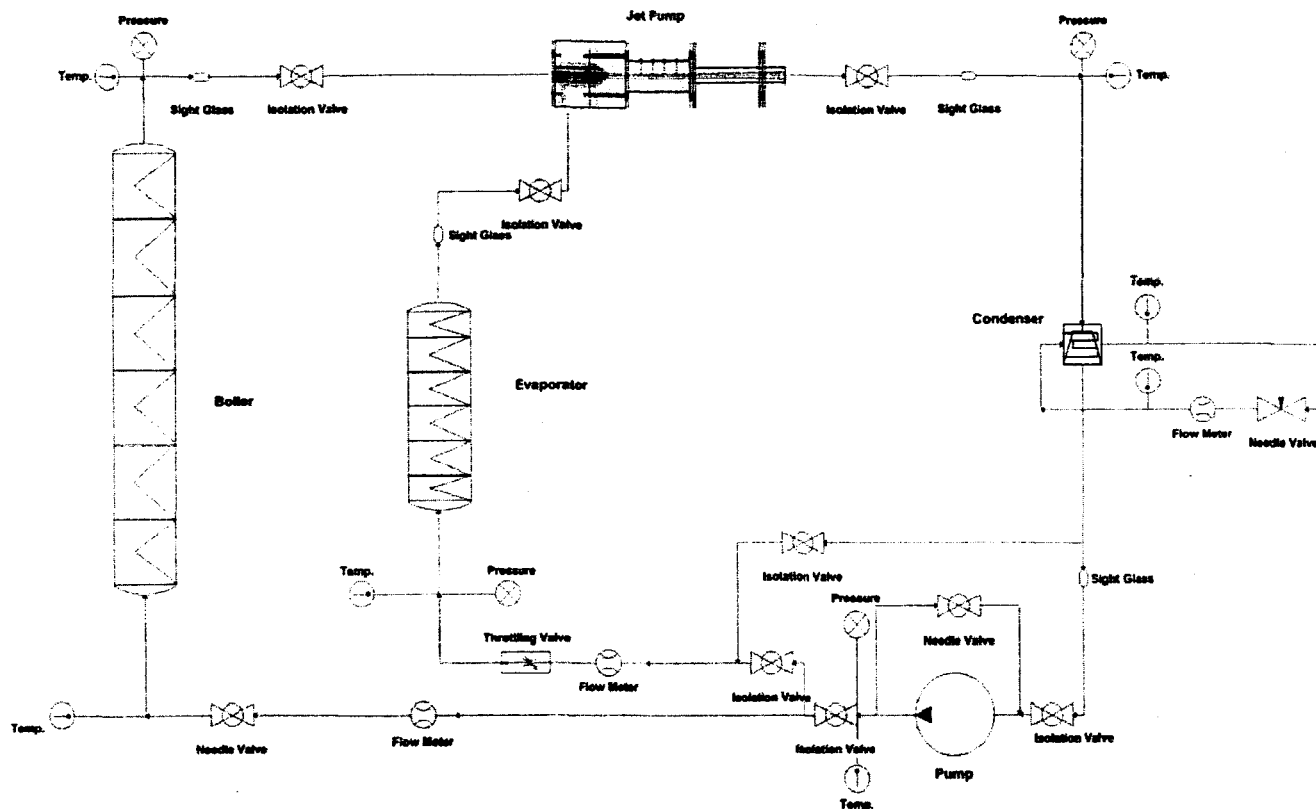


Figure 3. Schematic of the experimental testing apparatus

The arrangement of the aforementioned components used in conjunction with proper instrumentation allows the inlet conditions of the ejector to be varied over a wide range of conditions.

EJECTOR

Once the operating range of the testing apparatus was established, the ejector was designed. The ejector analysis is not included and the reader is referred to Nord et al. [2] for a detailed description of that part. Nord et al. [2] presented an iterative scheme that solves for the ejector exit state given the primary and secondary inlet states and the entrainment ratio. They then presented another iterative scheme to solve for all the other states in the SITMAP cycle given the output of the ejector analysis. The JetSit program referred to above was developed to efficiently perform the above ejector analysis and create performance graphs. JetSit's main functions are to calculate the ejector geometry and diffuser exit state and to use those results to calculate a solution to the SITMAP cycle. The program reads refrigerant properties from a data file, performs the necessary interpolations, uses the properties in the pump analysis schemes, and writes the results to a file. It should be noted that the JetSit code assumes constant-pressure mixing, whereas we use it for a guide for a constant-area mixing design. This is mentioned in more detail in the future work section. It should also be mentioned that JetSit is capable of analyzing ejector solutions for all flow regimes, including saturated flow.

The operating range of the testing apparatus was mapped into the inputs for the JetSit analysis. P_{si} was varied over the range of 0.15 MPa to 0.5 MPa, while X_{si} was varied from 0.5 to 1.0. The entrainment ratio ϕ was varied from 0.2 to 2.0. The primary inlet state was always in the superheated vapor region. Table 1 below shows some of the SITMAP inputs and their corresponding outputs. The ejector component outputs are the ejector compression ratio, the throat-to-exit area ratio of the primary nozzle, and the primary exit-to-secondary exit area ratio.

Table 1. Sample Inputs and Outputs of the Ejector Analyses

| Case | SITMAP Inputs | | | | | SITMAP Outputs | | |
|------|---------------|----------|----------|----------|--------|----------------|-----------------|-----------------|
| | T_{pi} | P_{pi} | X_{si} | P_{si} | ϕ | P_r | A_{nt}/A_{ne} | A_{nc}/A_{sc} |
| 1 | 130 | .60 | .75 | .15 | 1.1 | 1.65 | .694 | .222 |
| 2 | 130 | .60 | 1 | .15 | 1.1 | 1.57 | .694 | .194 |
| 3 | 130 | .60 | .75 | .15 | .2 | 2.7 | .694 | 1.223 |
| 4 | 130 | .60 | 1 | .15 | .2 | 2.65 | .694 | 1.067 |

Once the analysis has been performed over the range of specified conditions, the appropriate area ratios were determined.

Shown below in Fig. 4 is a schematic of the conceptual design of the ejector. The design is centered on the idea of a removable primary nozzle. In order to get multiple primary-to-secondary area ratios, multiple removable primary nozzles will need to be designed. The key to this design is to make it where the primary nozzle is easy to get to and easy to change. Making the nozzle easy to change will speed up the test phase.

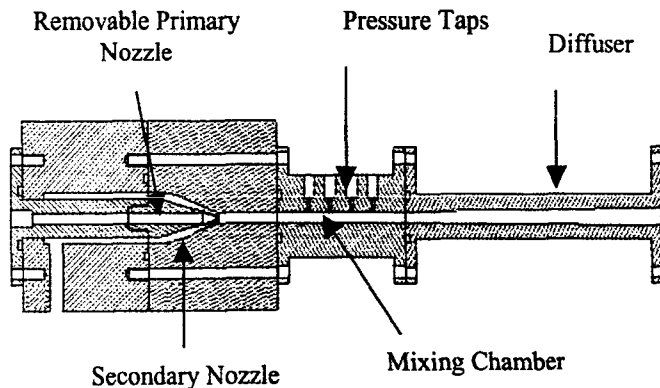


Figure 4. Ejector design

Once the basic ejector geometry has been fixed, the removable nozzle dimensions could be designed. This part of the design started by first fixing the mixing chamber diameter. Next the mixing chamber diameter was set equal to the outside diameter of the secondary nozzle, while the inside diameter of the secondary nozzle was set equal to the outside diameter of the primary nozzle. A schematic of this is shown in Figure 5. By using the above design geometry it is possible to achieve different area ratios A_{nt}/A_{ne} and A_{ne}/A_{se} by simply changing the primary nozzle. Using this technique, ten nozzles were designed to incrementally cover the desired range of area ratios.

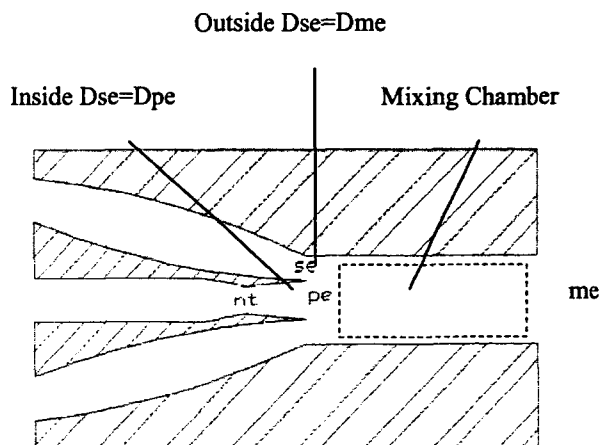


Figure 5. Constant-area ejector design

EXPERIMENTAL PROCEDURE

An experimental procedure has been developed in order to systematically test the ejector over the desired range of conditions. The procedure involves a test plan using the variable heat inputs along with a range of valve settings to achieve specified pressures and temperatures. This allows the pump to be tested over the widest range of inlet conditions possible. The procedure is to be repeated for every nozzle, so that the geometrical effects of the primary nozzle expansion ratio and the primary-to-secondary area ratio may be studied. The data obtained will be reduced using a generalized equation of state, so that the results will have maximum generality. Thus it is expected that the data obtained in this program will be applicable with reasonable accuracy to two-phase ejectors operating with other working fluids.

SUMMARY

An experimental rig has been designed in order to test constant-area ejector performance over a range of primary and secondary inlet conditions, concentrating on operation in the two-phase regime. The design allows P_{pi} to vary from 0.5 MPa to 0.83 MPa while P_{si} can be varied over the range of 0.15 MPa to 0.5 MPa. Since the heat input to both the primary and secondary flow is controlled, the fluid for both streams can be liquid, two-phase, or superheated vapor. In addition, several ejector geometry design variables may be adjusted, allowing for multiple ejector area ratios to be tested. All support structure and flow components have been acquired, and the test facility is in the final stages of assembly. The system has been designed to implement the SITMAP cycle, allowing a preliminary performance database to be developed upon testing. The flexibility of this experimental test rig will also allow a high-quality design database of the global performance parameters of two-phase ejectors to be obtained.

FUTURE WORK

The JetSit code will be modified from its current form in order to accommodate certain analytical needs. The first change involves matching code inputs with experimental inputs. Currently JetSit is a design-oriented code and will need to have an analysis mode added to it. The current design mode only takes the ejector inlet conditions as inputs and allows the ejector geometry to automatically adjust to its optimum design point. A new analysis mode will need to have the ejector geometry as well as the inlet state points as inputs. By having the geometry as an input a direct comparison between the theoretical and actual results for a given geometry can be made.

The second change that will need to be made involves the governing equations. Currently the JetSit code is based on a constant-pressure mixing ejector; whereas, in this experimental setup, the ejector is constant-area. The current form of the code was used only as a guide to get a range of viable area ratios. The main difference in the ejector analysis is found in the mixing chamber. In the case of constant-pressure mixing $P_{ne} = P_{se}$; this must be changed in order to account for the case where $P_{ne} \neq P_{se}$. Using a control volume approach and comparing the

momentum equation for each case help realize the differences in the ejector analysis. The constant-pressure control volume as shown in Fig. 1 yields Equation (1) and the constant-area control volume shown in Figure 5 yields Equation (2). In analysis mode, the modified JetSit code will implement Equation (2) in the mixing section.

$$(P_{ne} - P_{se})A_{ne} = -\dot{m}_p V_{ne} - \phi \dot{m}_p V_{se} + (1 + \phi) \dot{m}_p V_{me} \quad (1)$$

$$(P_{ne} - P_{me})A_{me} + (P_{se} - P_{ne})A_{se} = -\dot{m}_p V_{ne} - \phi \dot{m}_p V_{se} + (1 + \phi) \dot{m}_p V_{me} \quad (2)$$

A series of tests must also be conducted in order to characterize the experimental apparatus and to aid in the interpretation of the ejector performance data. The tests will be performed under certain operating conditions in order to get data in the specified regions. The results obtained from the tests will be used to validate the results from the ejector analysis. Shown below in Figs. 6 and 7 are examples of some graphical methods that will be used to compare the test results to the analytical model. A graph similar to Fig. 6 will be used to show the effects that varying the secondary inlet will have on the ejector pressure ratio for fixed ejector geometry, over a range of entrainment ratios.

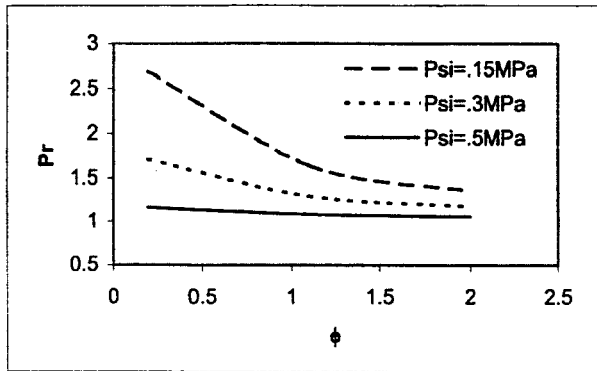


Figure 6. Performance curves of constant A_{ni}/A_{ne} , A_{ne}/A_{se} , T_{pi} , P_{pi} , and X_{si} for various design points

A graph similar to Fig. 7 will be used to show how the predicted ejector pressures ratio relates to the actual ejector pressure ratio. This will be used mainly for the validation of the model.

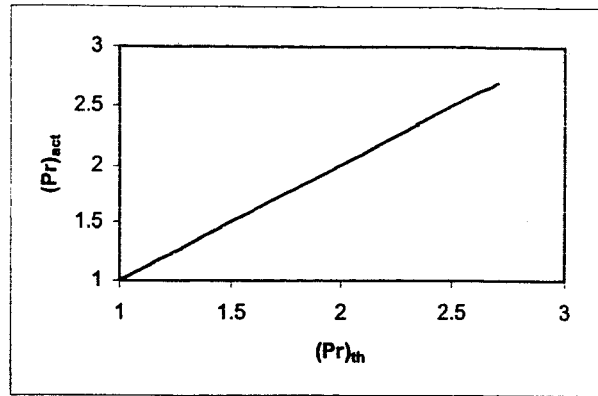


Figure 7. Predictions of performance relative to experimental findings

ACKNOWLEDGMENTS

This work was supported by NASA Glenn Research Center under grant number NRA-01-GRC-1 in the area of space power technology. Support from the Department of Mechanical and Aerospace Engineering at the University of Florida is also gratefully acknowledged.

REFERENCES

1. Sherif, S.A., Lear, W.E., Steadham, J.M., Hunt, P.L., and Holladay, J.B., "Analysis and Modeling of a Two-Phase Jet Pump of a Thermal Management System for Aerospace Applications," *International Journal of Mechanical Sciences*, Vol. 42, No. 2, February 2000, pp. 185-198.
2. Nord, J.W., Lear, W.E., and Sherif, S.A., "Design Analysis of a Heat-Driven Jet Pumped Cooling System for Space Thermal Management Applications," *AIAA Journal of Propulsion and Power*, Vol. 17, No. 3, pp. 566-570.
3. Freudenberg, K., Lear, W.E., Sherif, S.A., and Golliher, E.L., "Mass-Based Optimization of Thermal Management and Power Systems for Space Applications," *AIAA Journal of Propulsion and Power*, Vol. 18, No. 6, November-December 2002, pp. 1161-1169.
4. Kandil, S., Lear, W.E., and Sherif, S.A., "Performance of Jet-Pumped Cryogenic Refrigeration System," *40th AIAA Aerospace Sciences Meeting and Exhibit*, Reno, Nevada, January 14-17, 2002, AIAA Paper 2002-1031.
5. Bredikhin, V.V., Gorbenko, G.A., Nikonov, A.A., and Fairuzov, Y.V., "Mathematical Modeling of Thermo-Circulating Loops with Jet Pumps," *Hydrodynamic Processes in Multi-Phase Working Fluid Energy Plants*, Kharkov Aviation Institute, Kharkov, Ukraine, pp. 3-10 (in Russian), 1990.

6. Cunningham, R.G. and Dopkin, R.J., "Jet Breakup and the Mixing Throat Lengths for the Liquid Jet Pump," *ASME Journal of Fluids Engineering*, Vol. 96, No. 3, pp. 216-226, 1974.
7. Cunningham, R.G., "Liquid Jet Pumps for Two-Phase Flows," *ASME Journal of Fluids Engineering*, Vol. 117, No. 2, pp. 309-316, 1995.
8. Elger, D.F., McLam, E.T., and Taylor, S.J., "A New Way to Represent Jet Pump Performance," *ASME Journal of Fluids Engineering*, Vol. 113, No. 3, pp. 439-444, 1991.
9. Fabri, J. and Paulon, J., "Theory and Experiments on Air-to-Air Supersonic Ejectors," NACA-TM-1410, September 1958.
10. Fabri, J. and Siestrunk, R., "Supersonic Air Ejectors," *Advances in Applied Mechanics*, Vol. V, H.L. Dryden and Th. von Karman (editors), Academic Press, New York, 1958, pp. 1-33.
11. Fairuzov, Y.V. and Bredikhin, V.V., "Two Phase Cooling System with a Jet Pump for Spacecraft," *AIAA Journal of Thermophysics and Heat Transfer*, Vol. 9, No. 2, April-June 1995, pp. 285-291.
12. Holladay, J.B. and Hunt, P.L., "Fabrication, Testing, and Analysis of a Flow Boiling Test Facility with Jet Pump and Enhanced Surface Capability," Research Proposal, NASA Marshall Space Flight Center, Thermal and Life Support Division, Huntsville, Alabama, 1996.
13. Holmes, H.R., Geopp, J., and Hewitt, H.W., "Development of the Lockheed Pumped Two Phase Thermal Bus," AIAA Paper 87-1626, June 1987.
14. Jiao, B., Blais, R.N., and Schmidt, Z., "Efficiency and Pressure Recovery in Hydraulic Jet Pumping of Two-Phase Gas/Liquid Mixtures," *SPE Production Engineering*, Vol. 5, No.4, 1990, pp. 361-364.
15. Lear, W.E., Sherif, S.A., Steadham, J.M., Hunt, P.L., and Holladay, J.B., "Design Considerations of Jet Pumps with Supersonic Two-Phase Flow and Shocks," *AIAA 37th Aerospace Sciences Meeting*, Reno, Nevada, January 11-14, AIAA Paper 99-0461, 1999.
16. Marini, M., Massardo, A., Satta, A., and Geraci, M., "Low Area Ratio Aircraft Fuel Jet-Pump Performance with and without Cavitation," *ASME Journal of Fluids Engineering*, Vol. 114, No. 4, 1992, pp. 626-631.
17. Neve, R.S., "Diffuser Performance in Two-Phase Jet Pump," *International Journal of Multiphase Flow*, Vol. 17, No. 2, pp. 267-272, 1991.
18. Kakabaev, A. and Davletov, A., "A Freon Ejector Solar Cooler," *Geliotekhnika*, Vol. 2, No. 5, September 1966, pp. 42-48.
19. Chen, L.T., "Solar Powered Vapor-Compressive Refrigeration System Using Ejector as the Thermal Compressors," *Proceedings of the National Science Council*, No. 10, Part 3, pp. 115-132, 1977.
20. Lansing, F.L. and Chai, V.W., "Performance of Solar-Powered Vapor-Jet Refrigeration Systems with Selected Working Fluids," DSN Progress Report 42-44, Jet Propulsion Laboratory, 1978, pp. 245-248.
21. Chai, V.W. and Lansing, F.L., "A Thermodynamic Analysis of a Solar-powered Jet Refrigeration System," DSN Progress Report 41-42, Jet Propulsion Laboratory, 1977, pp. 209-217.
22. Abrahamsson, K., Jernqvist, A., and Ally, G., "Thermodynamic Analysis of Absorption Heat Cycles," *Proc. of the International Absorption Heat Pump Conference*, New Orleans, Louisiana, AES-Vol. 31, ASME, 1994, pp. 375-383.
23. Alefeld, G. and Radermacher, R., *Heat Conversion Systems*, CRC Press, Boca Raton, Florida, 1994.
24. Anderson, H., "Assessment of Solar Powered Vapor Jet Air-conditioning System," *International Solar Energy Congress and Exposition (ISES)*, Los Angeles, California, pp. 408, 1975.